

Article

The Impact of Fast-Rise-Time Electromagnetic Field and Pressure on the Aggregation of Peroxidase upon Its Adsorption onto Mica

Vadim S. Ziborov ^{1,2}, Tatyana O. Pleshakova ¹, Ivan D. Shumov ¹ , Andrey F. Kozlov ¹, Anastasia A. Valueva ¹, Irina A. Ivanova ¹, Maria O. Ershova ¹, Dmitry I. Larionov ¹ , Alexey N. Evdokimov ³, Vadim Yu. Tatur ³, Alexander I. Aleshko ⁴, Konstantin Yu. Sakharov ⁴, Alexander Yu. Dolgoborodov ², Vladimir E. Fortov ², Alexander I. Archakov ¹ and Yuri D. Ivanov ^{1,2,*}

- ¹ Institute of Biomedical Chemistry, Pogodinskaya Str., 10, 119121 Moscow, Russia; ziborov.vs@yandex.ru (V.S.Z.); t.pleshakova1@gmail.com (T.O.P.); shum230988@mail.ru (I.D.S.); afkozlow@mail.ru (A.F.K.); varuevavarueva@gmail.com (A.A.V.); i.a.ivanova@bk.ru (I.A.I.); motya00121997@mail.ru (M.O.E.); corvus.coraxnm@gmail.com (D.I.L.); alexander.archakov@ibmc.msk.ru (A.I.A.)
- ² Joint Institute for High Temperatures of the Russian Academy of Sciences, 125412 Moscow, Russia; aldol@ihed.ras.ru (A.Y.D.); fortov@ihed.ras.ru (V.E.F.)
- ³ Foundation of Perspective Technologies and Novations, 115682 Moscow, Russia; alxevd@yandex.ru (A.N.E.); v_tatur@mail.ru (V.Y.T.)
- ⁴ The All-Russian Research Institute for Optical and Physical Measurements Federal State Unitary Enterprise (VNIIOFI) of the Federal Agency for Technical Regulation and Metrology of the Russian Federation, 119361 Moscow, Russia; aleskho@vniiofi.ru (A.I.A.); sax-m12@vniiofi.ru (K.Y.S.)
- * Correspondence: yurii.ivanov.nata@gmail.com



Citation: Ziborov, V.S.; Pleshakova, T.O.; Shumov, I.D.; Kozlov, A.F.; Valueva, A.A.; Ivanova, I.A.; Ershova, M.O.; Larionov, D.I.; Evdokimov, A.N.; Tatur, V.Y.; et al. The Impact of Fast-Rise-Time Electromagnetic Field and Pressure on the Aggregation of Peroxidase upon Its Adsorption onto Mica. *Appl. Sci.* **2021**, *11*, 11677. <https://doi.org/10.3390/app112411677>

Academic Editors: Dayun Yan, Roberto Zivieri and Heping Li

Received: 7 October 2021

Accepted: 2 December 2021

Published: 9 December 2021

Publisher's Note: MDPI stays neutral with regard to jurisdictional claims in published maps and institutional affiliations.



Copyright: © 2021 by the authors. Licensee MDPI, Basel, Switzerland. This article is an open access article distributed under the terms and conditions of the Creative Commons Attribution (CC BY) license (<https://creativecommons.org/licenses/by/4.0/>).

Abstract: Our present study concerns the influence of the picosecond rise-time-pulsed electromagnetic field, and the impact of nanosecond pulsed pressure on the aggregation state of horseradish peroxidase (HRP) as a model enzyme. The influence of a 640 kV/m pulsed electromagnetic field with a pulse rise-time of ~200 ps on the activity and aggregation state of an enzyme is studied by the single-molecule atomic force microscopy (AFM) method. The influence of such a field is shown to lead to aggregation of the protein and to a decrease in its enzymatic activity. Moreover, the effect of a shock wave with a pressure front rise-time of 80 ns on the increase in the HRP aggregation is demonstrated. The results obtained herein can be of use in modeling the impact of electromagnetic and pressure pulses on enzymes and on whole living organisms. Our results are also important for taking into account the effect of pulsed fields on the body in the development of drugs, therapeutic procedures, and novel highly sensitive medical diagnosticums.

Keywords: horseradish peroxidase; atomic force microscopy; protein aggregation; shock wave; pulsed electromagnetic field

1. Introduction

Biological systems are often subjected to external influences. Electromagnetic fields are now actively used in both industry and everyday life [1]. Moreover, the use of microwave electromagnetic radiation for medical applications is discussed [2–5]. High pressure is another type of external impact, which also takes place in nature, and can thus affect protein structure [6]. Such external influences are known to be able to affect the protein structure [6,7]—including the aggregation state—and other physicochemical properties of proteins. These properties of proteins, in their turn, determine the proper functioning of the entire organism. This is why studying the effect of electromagnetic and pressure fields on proteins represents an actual problem of modern life science.

Regarding the aggregation state of proteins, in animals and humans, protein aggregates can have either positive or negative effects. The positive effect consists of providing

proper functioning of the body; for instance, myeloperoxidase functions in dimeric form [8], formed by functionally independent monomeric units joined by a single disulfide bond at Cys153 [9]. Another example is glutathione peroxidase, which participates in oxidative stress regulation and is functionally active in tetrameric form [10].

The negative effect of protein aggregation manifests itself in the form of the development of various pathologies in the body caused by the formation of protein aggregates. Namely, protein aggregation is known to be a cause of cardiovascular diseases [11]. Furthermore, protein aggregation was reported to be associated with cancer in humans: Xu et al. [12] reported that aggregation processes, which involve mutant p53 protein, are associated with the development of cancer, which could thus be considered as aggregation-associated disease. This was confirmed in the research performed by other authors [13–15]. Another well-known fact is that the formation of amyloid aggregates in the brain was considered to lead to Parkinson's [16] and Alzheimer's [16–18] diseases. In this connection, it should be, however, emphasized that certain proteins in amyloid form are relevant for proper brain functioning: therefore, in mammals' brain, FXR1 protein, which regulates memory and emotions, is functioning in amyloid form [16].

Medicinal agents, intended for the treatment of diseases caused by protein aggregation, are often non-specifically disrupting the protein aggregates. During such a non-specific therapy, however, not only the target pathology-associated protein aggregates but also the ones required for proper body functioning, can be destroyed. In this connection, the revelation and investigation of factors influencing protein aggregation, the development of methods for the assessment of this influence, and the development of novel approaches providing specific correction of protein aggregation, represent important tasks of modern biomedical research aimed at maintaining human health.

Regarding magnetic (MFs) and electromagnetic fields (EMFs), a lot of attention is given to these fields with relatively long rise-times. Both extremely low frequency (20 to 75 Hz [1,19–21]) and microwave frequency EMFs [22–24] are known to influence protein structure and/or functionality. Regarding protein structure changes, irradiation in 940 MHz circularly polarized EMF was shown to cause partial unfolding of adult hemoglobin [22]. Lopes et al. [23] reported that 0.5 h-long microwave irradiation (at a temperature of 60 °C and radiation power of 60 W) of horseradish peroxidase leads to significant (~80%) loss in its enzymatic activity. Moreover, Latorre et al. have demonstrated that just 30 s irradiation of a sample containing red beet peroxidase and polyphenoloxidase in 2450 GHz EMF (at 450 W microwave power) causes a very significant decrease in their enzymatic activity: namely, these authors observed 15-fold and 100-fold decrease in the activity of red beet peroxidase and polyphenoloxidase, respectively [24]. The influence of EMF with extremely low frequency (ELF-EMF) can either stimulate or suppress the activity of enzymes. Therefore, Morelli et al. found that a number of membrane-associated enzymes (alkaline phosphatase, acetylcholinesterase from blood cell membranes, acetylcholinesterase from synaptosomes, phosphoglycerate kinase, and adenylate kinase) lose their activity upon the influence of a 75 Hz ELF-EMF, while other enzymes (CaATPase, Na/K ATPase, and succinic dehydrogenase) are virtually insensitive to such an influence [19]. Thumm et al. observed a 2-fold increase in the activity of cAMP-dependent protein kinase in human skin fibroblasts after 1 h exposure to 20 Hz ELF-EMF (7–8 mT) [20]. Wasak et al. demonstrated that the enzymatic activity of horseradish peroxidase (HRP) can either increase or decrease after its exposure to an extremely low frequency (1 to 50 Hz) rotating MF, depending on the MF parameters [25]. Caliga et al. [21] observed a ~2-fold decrease in the HRP catalytic efficiency after its incubation in a 50 Hz (2.7 mT) ELF-EMF, while a 100 Hz (5.5 mT) ELF-EMF had virtually no effect on the enzyme. Modulation of the activity of enzymes by MFs can be explained by the interaction of the MF with the 3D structure of the protein [26]. The number of papers reporting the effects of electric and/or electromagnetic fields with picosecond rise-times on biological systems is quite low. Considering the cellular level, Gao et al. [27] reported that an extremely high intensity pulsed electric field with 150 ps rise-time is able to permeabilize biological cells. In the

works considering the influence of pulsed electromagnetic fields at the protein level, the studied range of pulse rise-times is limited to nanoseconds [28]. Application of pulsed electromagnetic fields (PEMF) with nanosecond rise-times was demonstrated to enhance the sensitivity of diagnostic systems [29]. Moreover, the possibility of the use of non-thermal effects of low-power (from 10^{-5} to 10^{-3} W/cm²) sub-nanosecond pulsed radiation (with a rise-time of 200 ps) for cancer therapy was reported [3]. Studies on the application of microwave imaging for cancer diagnosis are also reported [2,4,5]. In this connection, studying the effect of pulsed non-thermal electromagnetic radiation on enzymes represents an important task for both fundamental and applied research, including medical and diagnostic applications [3]. Sinusoidal electromagnetic fields of GHz frequency were reported to influence the activity of heme-containing enzymes [28]. We are, however, not aware of any studies reporting such an influence from pulsed electromagnetic fields with shorter (picosecond) rise-times; accordingly, additional research is required to investigate whether such fields have an influence on enzymes.

Regarding pressure fields, they are also known to influence the structure and functionality of proteins [6] and enzymes [6,30–33]. Similar to electromagnetic radiation, the mechanical pressure, acting on biological objects, can be constant (hydrostatic) [6,30] or pulsed. The effects of hydrostatic pressure on enzyme systems were extensively studied previously. So, G. Hui Bon Hoa et al. [30] studied the impact of a constant 1000 to 3000 bar pressure on the properties of heme-containing enzymes and demonstrated that such an impact can lead to a change in their structure and functional activity. The latter case is very interesting with regard to studying electron transport systems, which participate in the metabolism of various compounds in the body [30]. In their review, Eisenmerger and Reyes-De-Corcuera [31] discuss the effect of high (up to hundreds MPa) hydrostatic pressure on various types of enzymes (oxidoreductases, transferases, hydrolases, and lyases). These authors emphasize that in general, high pressure can help to stabilize enzymes against thermal denaturation, but at the same time, the enzymatic activity can be either increased or suppressed depending on each specific case. Andreou et al. [32] and Akazawa et al. [33] demonstrated that the sensitivity to high pressure is the individual characteristic of each enzyme. In experiments performed by Andreou et al., the enzymatic activity of polygalacturonase decreased rapidly (down to complete inactivation after 10 min treatment) upon the action of high (up to 500 MPa) pressure, while pectinmethylesterase retained ~70% of its initial enzymatic activity even after 20 min treatment at 800 MPa [32]. Akazawa et al. observed a decrease in β -glucosidase and lipase activities at 0.1 MPa and higher pressures, while α -amylase exhibited higher activity at high (400 MPa) pressure; these authors also demonstrated pressure-induced activation of lumbrokinase at 200 MPa and higher (up to 500 MPa) pressures [33]. Once again, in the above-mentioned papers [6,30], studies of the pressure impact on proteins are limited to the cases with constant pressure. In this regard, studying the influence of fast rise-time-pulsed pressure impacts on proteins represents an actual direction of research.

Peroxidase enzyme systems are known to perform important functions in various metabolic processes. Peroxidases pertain to heme-containing enzymes, which are well represented in plant and animal tissues [34]. This provokes a great interest in studying this class of enzymes. In humans, myeloperoxidase participates in atherogenesis [8] and in oxidative stress [10]. For these considerations, a peroxidase has been employed in our present study as a model object. Namely, horseradish peroxidase, which is comprehensively characterized in the literature, is often employed as a model object in studies of a wide class of peroxidases. HRP represents a glycoprotein with a molecular weight of about 40 to 44 kDa [35,36], which can form aggregates [37]. HRP catalyzes the oxidation of many organic and inorganic compounds by hydrogen peroxide [38]. It is known that HRP represents a D-isomer, whose structure includes 77% α -helices and 12% β -sheets [39]; its macromolecule also includes 18% to 27% of carbohydrate chains, which stabilize the protein structure [36,40,41]. Accordingly, the structure of this enzyme is chiral (or more exactly, pseudo-chiral).

AFM allows one to visualize and measure the functional activity of single enzyme molecules [42,43], thus representing a very convenient tool for the determination of their aggregation state. This is quite useful for single-molecule enzymology. For this reason, in our research, atomic force microscopy (AFM) was employed to study the effect of external factors on HRP aggregation. Previously, AFM was employed to study the formation of various protein complexes [44–53]. In parallel, in our present study, a commonly used spectrophotometry-based technique was employed to estimate the enzymatic activity of HRP in solution.

Our present work is aimed at the AFM investigation of the influence of short (sub-nanosecond and nanosecond) electromagnetic (640 kV/m) and pressure (10 atm) pulses on protein aggregation. The pulse rise-time was ~200 ps in the case of PEMF, and 80 ns in the case of the pulsed pressure field. In the literature, such pulses were called ultra-short electromagnetic pulses (USEMP) [54]. The parameters of the electromagnetic field have been chosen based on the above-discussed factors, since such electromagnetic field characteristics are interesting from a practical point of view for diagnostic applications (for instance, for microwave imaging of cancer [4,5]). Accordingly, as discussed above, it is important to find out whether electromagnetic fields with such characteristics have an effect on enzymes. And herein we have studied the influence of PEMF using HRP as a model enzyme.

It has been demonstrated that an increased aggregation of the HRP molecules is observed after the exposure of its solution to PEMF. Moreover, the enzymatic activity of HRP also decreased considerably after the irradiation of the enzyme solution in PEMF. We have also demonstrated that a pressure jump, induced by the action of a fast rise-time (of the order of 80 ns) shock wave, leads to an aggregation of the protein. The influence of the pressure jump and the pulsed electromagnetic field on the protein aggregation state is discussed. It has been considered that, according to the literature [55], protein aggregation can lead to a change in circular dichroism spectra, i.e., influences stereochemical properties of the protein molecules. This aspect is interesting due to the fact that chirality and specific stereochemical properties of biological molecules are commonly occurring in living organisms, however, the nature of this phenomenon is still unknown.

The results obtained herein can find their application in the development of models describing the interaction of electromagnetic and pressure fields with enzyme systems and with whole organisms. The data obtained can also be used in further studies aimed at the development of safety standards regarding the practical use of electromagnetic fields. Our results should also be taken into account in the development of novel highly sensitive diagnosticums, intended for the revelation of diseases associated with protein aggregation, and new medicinal agents intended for the treatment of these pathologies.

2. Materials and Methods

2.1. Chemicals and Protein

Peroxidase from horseradish (HRP; lyophilized powder) was purchased from Sigma (St. Louis, MO, USA). 2,2'-azino-bis(3-ethylbenzothiazoline-6-sulfonate) (ABTS) was purchased from Sigma. Disodium hydrogen orthophosphate (Na_2HPO_4), citric acid, and hydrogen peroxide (H_2O_2) were purchased from Reakhim (Moscow, Russia). All solutions were prepared using deionized ultrapure water (with $18.2 \text{ M}\Omega \times \text{cm}$ resistivity) obtained with a Simplicity UV system (Millipore, Molsheim, France).

We performed all our AFM experiments with $0.1 \mu\text{M}$ (10^{-7} M) HRP solution in 2 mM potassium phosphate buffer (pH 7.4). This solution was obtained by sequential tenfold dilution of $10 \mu\text{M}$ HRP stock solution; the latter was obtained by dissolving 1 mg of initial HRP preparation in 2.5 mL of deionized ultrapure water. The solutions under study were placed into standard 1.5 mL test tubes.

2.2. Experimental Setup for the Study of the Effect of the PEMF

The experimental setup was analogous to that described in detail by Sokolov et al. [56]. The setup represented an ultra-short electromagnetic pulse emitter, which comprised of a semiconductor-based high-voltage pulse generator (HVPG; FID GmbH, Burbach, Germany) and an antenna-feeder device (AFD), based on an array of 500 mm-long transverse electromagnetic (TEM) horn antennas. The working area, where the samples to be irradiated were placed, was located within the antenna mouth, as shown in Figure 1A.

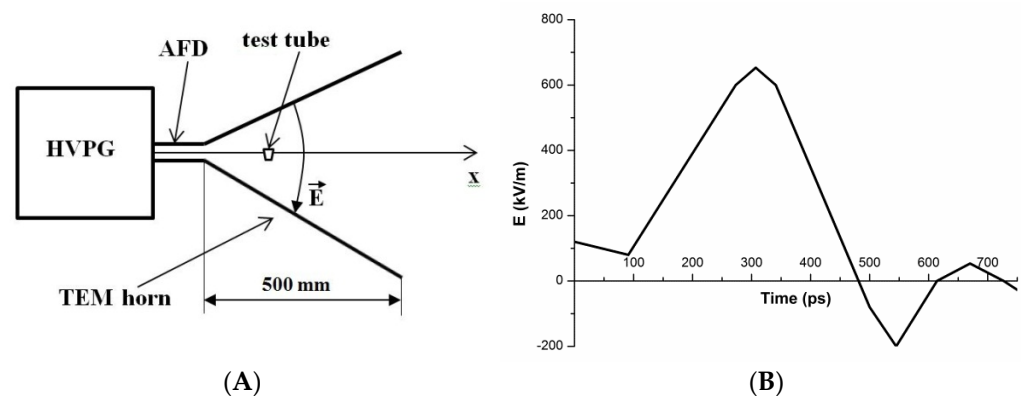


Figure 1. Schematic representation of the working area of the PEMF experimental setup (A); and oscillogram of the ultra-short electromagnetic pulses recorded within the antenna mouth in the point, where the test tube with the PEMF-irradiated solution was placed (B). In A, the thin-end arrows indicate the main units of the experimental setup: the HVPG (high-voltage pulse generator), the AFD (antenna-feeder device), the test tube containing the sample to be irradiated, and the TEM horn antenna. \vec{E} is the direction of the electric field strength vector, indicated by the thick-end arrow. The length of the TEM horn antenna is 500 mm.

The USEMP parameters were controlled with an IPPL-L converter of pulsed electric field strength (VNIIOFI, Moscow, Russia) [57–59].

The HVPG was intended for the excitation of the antenna array. The HVPG output was matched with the input of the antenna array. The dimensions of the working area were 400×500 mm.

In the working area of the emitter, the intensity of the pulsed electric field was measured. The pulses were recorded with an IPPL-L converter (conversion factor 5.11×10^{-4} V/(V/m), transient characteristic rise-time 5 ps, transient characteristic duration 4.6 ns), and a stroboscopic oscillograph (50 GHz bandpass). Figure 1B displays an oscillogram of the ultra-short electromagnetic pulses recorded within the antenna mouth in the point, where the test tube—with the solution to be irradiated—was placed.

A test tube, containing $0.1 \mu\text{M}$ (10^{-7} M) HRP solution in 2 mM potassium phosphate buffer (pH 7.4), was placed within the working area of the emitter (Figure 1A). The strength of the pulsed electromagnetic field at this point was 640 kV/m, while the pulse repetition rate was 16 Hz.

The energy supplied to the HRP enzyme solution was calculated using the equation [3]:

$$P(t) = [E(t) \times H(t)] = \frac{E^2(t)}{377} \quad (1)$$

where $E(t)$ and $H(t)$ are the instantaneous values of the strength of the electric and magnetic fields, respectively. The transition only to the instantaneous value of the electric field is valid for losses in a medium, where the ratio $E/H = 377$ (characteristic impedance of vacuum) is observed. The energy W , supplied to the irradiated object with the area S in one pulse, is calculated using the following equation:

$$W = S \int_0^T \frac{E^2(t)}{377} dt \quad (2)$$

The average power supplied to the area S depends on the pulse repetition rate F as follows:

$$\langle P \rangle = W \cdot F \quad (3)$$

Based on the calculation technique described in [3], given $E = 640 \text{ kV/m}$, one can obtain that the energy supplied with one pulse makes up $1.3 \times 10^{-4} \text{ J}$, while the average power for a period at 16 Hz frequency amounts to $2.1 \times 10^{-3} \text{ W}$.

2.3. Experimental Setup for the Study of the Effect of the Shock Wave

The shock wave was generated using an ISTRA conventional stainless steel high-vacuum shock tube with a diameter of 108 mm, schematically shown in Figure 2 [60,61].



Figure 2. Schematic representation of an ISTRA conventional shock tube experimental setup. Numbers indicate the main elements of the setup: 1 is the high-pressure chamber; 2 is the destructible copper membrane; 3 is the low-pressure chamber; 4 is the measuring section of the low-pressure chamber containing pressure sensors; 5 is the sample with a test tube containing a solution of HRP enzyme placed at the end of the shock tube.

To generate a shock wave in the gas, which turned into a shock compression wave of a sample containing a test tube with a solution of the enzyme HRP, a conventional “ISTRA” shock tube made of stainless steel with an inner diameter of 108 mm was used. The pressure behind the shock wave front was determined by the measured values: the initial gas pressure, its temperature, and the velocity of the front of the incoming shock wave, which was measured by four piezo sensors installed at known distances from the end of the shock tube in its measuring section. The initial gas pressure, its temperature, and the pressure of rupture of the membrane between the high-pressure chamber and the low-pressure one were chosen in such a way that the pressure behind the shock wave, reflected from the sample, was 10 atm, and it lasted about 4 ms before the arrival of the rarefaction wave. The sample, with the object under study, was placed at the end of the shock tube in the measuring section. The sample was an assembly of a metal flat cylinder, into which a test tube with $0.1 \mu\text{M}$ (10^{-7} M) HRP solution in 2 mM potassium phosphate buffer (pH 7.4) was placed, and the free space in the cylinder was filled with cured epoxy resin. The one-dimensional shock wave propagating in the measuring section interacted with the flat end face of the sample perpendicular to the normal to its surface. The characteristic profile of the shock wave front in the gas was measured by the laser Schlieren method [61]. The pressure rise-time was about 80 to 100 ns.

2.4. AFM Experiments and Sample Preparation

The experiments were carried out by the direct surface adsorption method [45]. In this method, the protein objects to be studied adsorb onto the AFM substrate surface during its incubation in the analyzed solution. Herein, mica sheets (SPI, West Chester, PA, USA) were employed as AFM substrates with a hydrophilic surface. The samples for the AFM measurements were prepared as follows. A $7 \times 15 \text{ mm}$ piece of mica sheet was immersed into 800 μL of the analyzed $0.1 \mu\text{M}$ (10^{-7} M) HRP solution in 2 mM potassium phosphate buffer (pH 7.4), which was either exposed (working experiment) or not exposed to the field (control experiment). The mica substrate was incubated in the analyzed solution for 10 min in a shaker (Thermomixer Comfort, Eppendorf, Germany) at 600 rpm and room temperature. After the incubation, each substrate was first rinsed with the ultrapure distilled water and then scanned by AFM in air at 60% air humidity. Under such conditions, biological macromolecules were reported to retain their native structure owing to the presence of a water layer on the surface of bare mica [62].

The protein concentration used in the experiments was dictated by inherent limitations of the AFM-based technique: at higher concentrations the molecules under study formed continuous layers on the mica substrate, making the identification of individual objects impossible. It should be emphasized that the concentration studied is still relevant physiologically: the concentration of glutathione peroxidase in human plasma was reported to be $\sim 10^{-7}$ M [10].

The mica substrate surface with adsorbed HRP was visualized by AFM. AFM allows one to measure the heights of the visualized biological macromolecules with high (down to 0.1 nm) resolution [42,43]. At the same time, the lateral dimensions of the AFM images of the visualized objects can be broadened due to the effect of convolution of the probe and the objects under study, as the AFM tip has a certain curvature radius [63]. For this reason, herein, the height of AFM images was used as a criterion for the estimation of a change in the size of the visualized objects. All AFM experiments were performed in tapping mode with a Titanium multimode atomic force microscope (NT-MDT, Moscow, Russia), equipped with NSG10 cantilevers ("TipsNano", Zelenograd, Russia; 47 to 150 kHz resonant frequency, 0.35 to 6.1 N/m force constant). The calibration of the microscope by height was carried out on a TGZ1 calibration grating (NT-MDT, Zelenograd, Russia; step height 21.4 ± 1.5 nm). The total number of measured particles in each sample was no less than 200, and the number of frames for each sample was no less than 10. The density of protein distribution with height, $\rho(h)$, was calculated as:

$$\rho(h) = (N_h/N) \times 100\% \quad (4)$$

where N_h is the number of imaged objects with height h , and N is the total number of imaged objects [52]. In the protein-free experiments, when the mica substrates were incubated in protein-free ultrapure water, no objects with a height exceeding 0.5 nm were visualized.

Similar to [52], to correctly compare the data obtained in different experiments, the number of objects, visualized in each experiment, was normalized per a $400 \mu\text{m}^2$ area, and the number of visualized objects was accordingly calculated using the following equation:

$$N_{norm} = (N \times 400) (n \times a^2) \quad (5)$$

where N_{norm} is the number of objects per $400 \mu\text{m}^2$, N is the total number of particles visualized on all n AFM scans obtained in the experiment, and a is the side dimension of each AFM scan (in our experiments, the area of each scan was $2 \times 2 = 4 \mu\text{m}^2$).

2.5. Estimation of HRP Enzymatic Activity

HRP activity was estimated by conventional spectrophotometry as described in our previous studies [64,65], following the technique reported by Sanders et al. [66]. Briefly, ABTS was employed as a reducing substrate. Thirty microliters of 10^{-7} M HRP solution was added into a 3 mL quartz cuvette (pathlength 1 cm, Agilent, Technologies Deutschland GmbH, Waldbronn, Germany) containing 2.96 mL of 0.3 mM ABTS solution in phosphate-citrate buffer (51 mM Na_2HPO_4 , 24 mM citric acid, pH 5.0) and thoroughly stirred. In this way, the final HRP concentration in the cuvette was 10^{-9} M. Finally, 8.5 mL of 3% (w/w) H_2O_2 were added into the cuvette. The rate of change in solution absorbance was measured at 405 nm wavelength with an Agilent 8453 UV-Visible spectrophotometer (Agilent Technologies Deutschland GmbH, Waldbronn, Germany). Spectrum acquisition was initiated immediately upon the addition of H_2O_2 .

3. Results

The influence of the electromagnetic field and pressure pulses on the aggregation of HRP enzyme protein has been studied.

3.1. AFM Study of the Effect of Pulsed Electromagnetic Field

Figure 3 displays typical AFM images obtained upon AFM scanning of the surface of mica substrate after its incubation in working and control solutions of HRP, which were irradiated and not irradiated in the pulsed electromagnetic field, respectively.

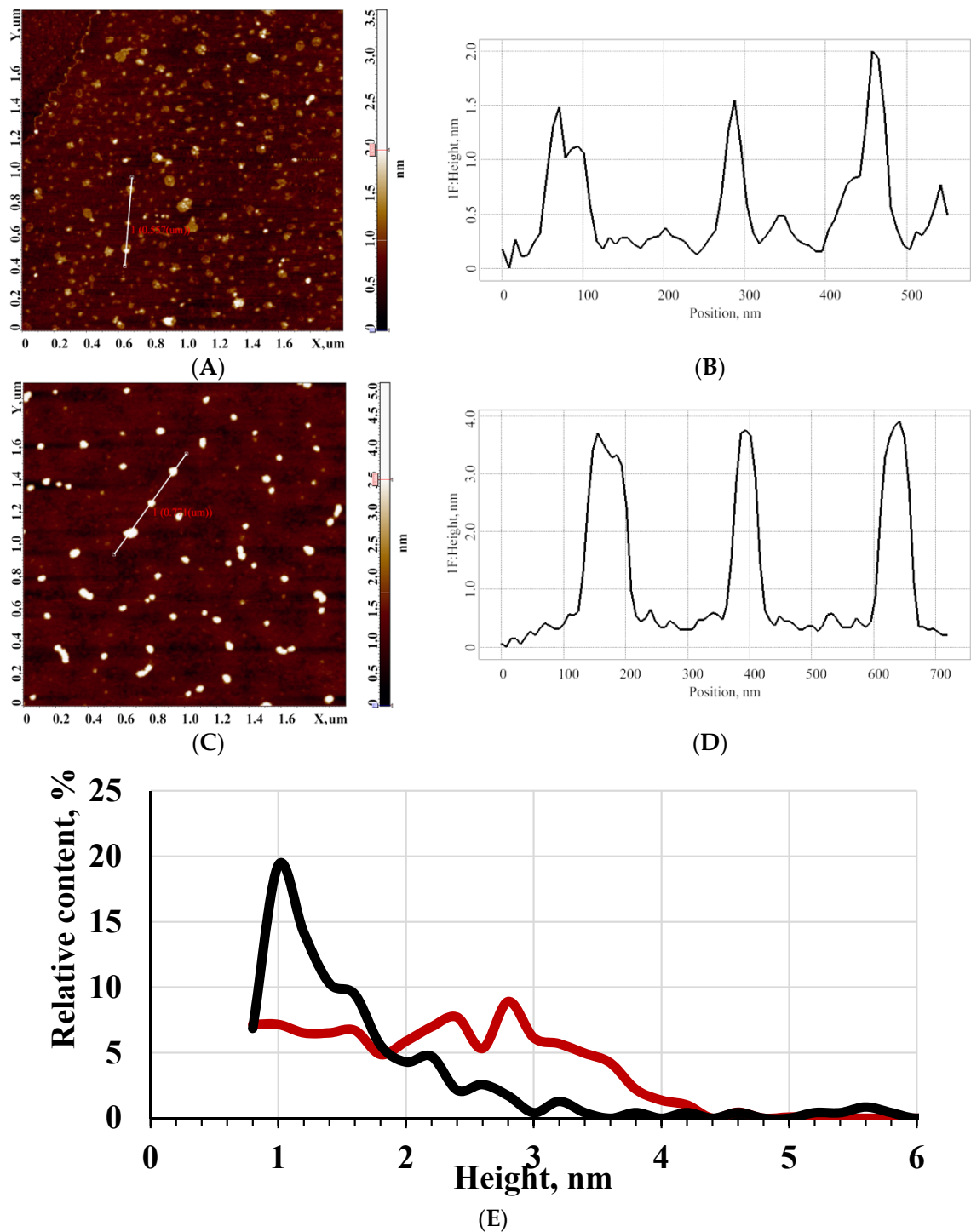


Figure 3. Results of AFM study of the effect of PEMF on the HRP aggregation. (A–D) Typical AFM images (A,C) and cross-section profiles (B,D) of the surface of mica substrate obtained after its incubation in 0.1 μM aqueous HRP solution, which was either not irradiated (A,B) or irradiated (C,D) in PEMF. The cross-section profiles correspond to the lines in the respective AFM images. (E) Distribution plots of the AFM-visualized objects with height $\rho(h)$, obtained for the PEMF-irradiated (red curve) and for the control HRP solution (black curve).

Panel (A) displays the image obtained in the control experiment. In this experiment, no electromagnetic impact on the analyzed enzyme solution was performed. As seen from Figure 3A,B, in the case of the absence of an electromagnetic field impact on the protein solution, it adsorbs onto the substrate surface in the form of compact objects, whose height makes up 1 to 2 nm. After processing the AFM data obtained, a distribution of the visualized objects with height $\rho(h)$ was plotted. The $\rho(h)$ distribution plot is shown in Figure 3E (black curve). The $\rho(h)$ distribution curve indicates that the maximum number of the visualized objects have a height of about (1.0 ± 0.2) nm, while the width at half-height makes up 0.8 nm.

The molecular weight of HRP is known to be 40 to 44 kDa [35,36]. Moreover, in previous studies, it was demonstrated that proteins of similar molecular weight—for instance, monomers of various cytochromes P450—also have a height of about 1 to 2 nm [67,68]. For these considerations, we have concluded that the objects with a height of 1 to 2 nm, observed during AFM scanning, can be attributed to HRP monomers. At the same time, the $\rho(h)$ distribution curve has an inflection point near 1.4 nm, which indicates a nonmonotonic decrease in the $\rho(h)$ function in this area. This indicates a contribution of aggregate objects to the right wing of the distribution at $h > 1.6$ nm. Thus, the presence of HRP on the mica substrate surface is observed in the form of a mixture of monomers and aggregates.

Figure 3C,D displays typical AFM images of the mica surface with HRP molecules, adsorbed from the solutions irradiated in the pulsed electromagnetic field for 40 min.

As seen from Figure 3C,D, the appearance of objects with 3 to 4 nm height is observed on the substrate surface after its incubation in HRP solution, which was irradiated in PEMF for 40 min—in contrast to the case with the control solution. After processing the AFM data, a $\rho(h)$ distribution was plotted analogously to the case with the control experiment. The resulting distribution plot is shown in Figure 3E (red curve). The obtained $\rho(h)$ curve indicates that the maximum number of objects, visualized in the case of PEMF-irradiated HRP solution, have a height of about (2.8 ± 0.2) nm, while the width at half-height makes up 3.5 nm. That is, after the irradiation of HRP enzyme solution in PEMF, the shape of the $\rho(h)$ distribution curve changes significantly—in comparison with that obtained for the control HRP solution. The objects with heights from 2 to 4.5 nm, visualized on the surface of the substrate incubated in PEMF-irradiated solution, can be attributed to HRP aggregate structures. Thus, one can clearly observe an increase in the content of the aggregate structures adsorbed onto the mica surface from the HRP solution after its exposure to PEMF.

3.2. AFM Study of the Effect of Pulsed Pressure

AFM images of HRP, adsorbed onto the mica surface from its solutions before and after the impact of the shock wave, were obtained, and corresponding distributions of the visualized objects with height were plotted after processing the AFM images.

Figure 4 displays typical AFM images, and the $\rho(h)$ distribution plots obtained for HRP adsorbed from solutions before and after the impact of the shock wave. The curves shown in Figure 4 indicate a slight increase in the number of objects with a height from 1.5 to 6 nm after the shock wave impact—in comparison to the case with control experiments. The appearance of larger objects indicates that a tendency of HRP protein to adsorb onto mica with an increase in the degree of aggregation occurs after the impact of the shock wave on its solution.

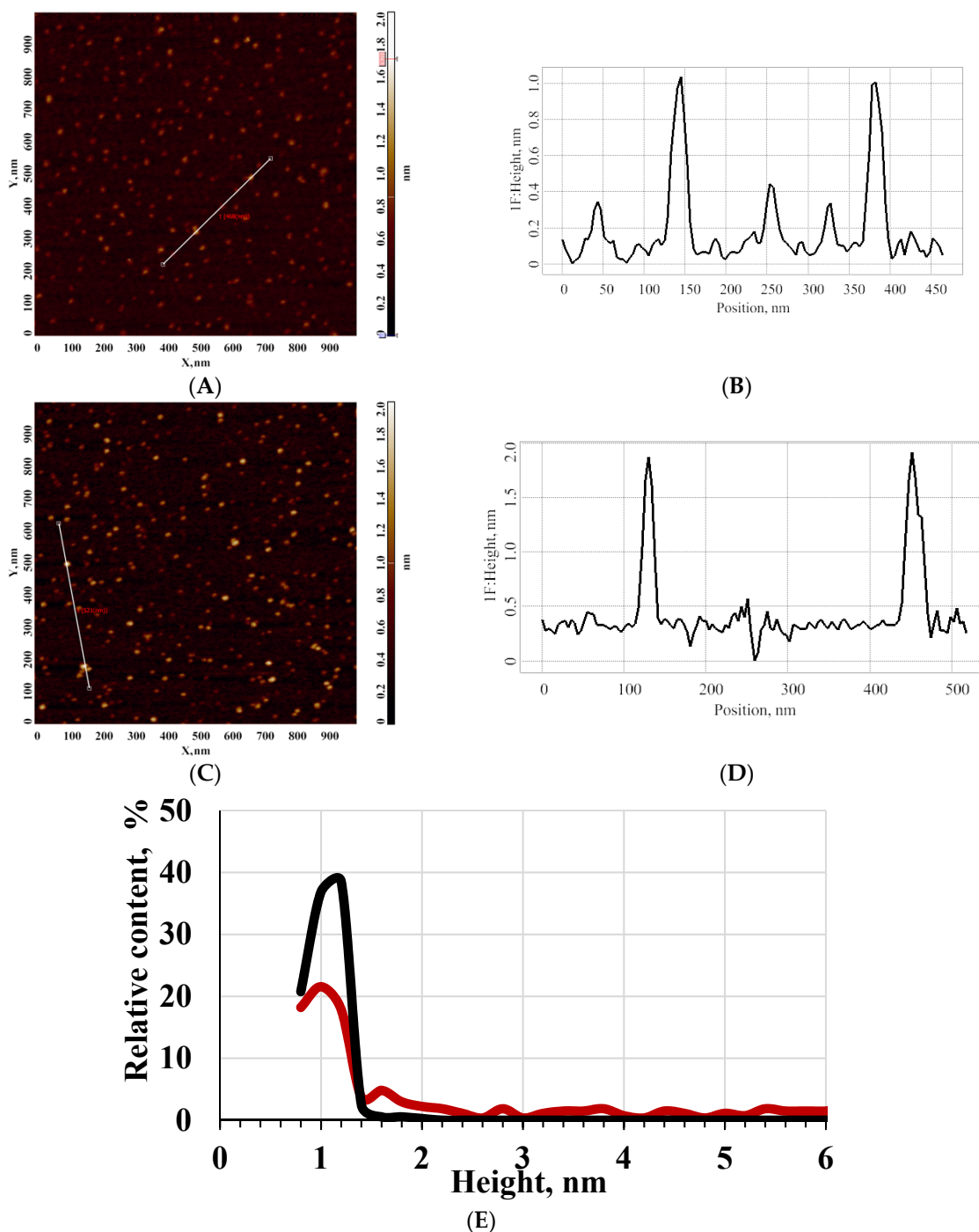


Figure 4. Results of AFM study of the effect of the shock wave impact on the HRP aggregation. Representative AFM images (A,C) and cross-section profiles (B,D) of the surface of mica substrate obtained after its incubation in 0.1 μM aqueous HRP solution, which was either not subjected (A,B) or subjected (C,D) to the shock wave impact. The cross-section profiles correspond to the lines in the respective AFM images. (E) Distribution plots of the AFM-visualized objects with height $\rho(h)$, obtained for the solution subjected to the shock wave impact (red curve) and for the control HRP solution (black curve). Experimental conditions: the pressure behind the reflected shock wave was 10 atm for 4 ms, the rise-time of the shock wave front was about 80 nsec.

3.3. Spectrophotometry-Based Estimation of the Effect of Pulsed Electromagnetic and Pressure Field on the Enzymatic Activity of HRP

The enzymatic activity of HRP was estimated by monitoring the time dependencies of the solution absorbance at 405 nm ($A_{405}(t)$) upon the reaction of HRP with ABTS substrate employing a technique developed by Sanders et al. [66]. These spectrophotometric measurements were performed for both the HRP sample, exposed to a 640 kV/m PEMF with a pulse repetition rate of 16 Hz for 40 min, and the control HRP sample, which was not exposed to PEMF. That is, the HRP solutions studied by spectrophotometry and those studied by AFM were treated under the same conditions. Figure 5 displays the obtained $A_{405}(t)$ curves.

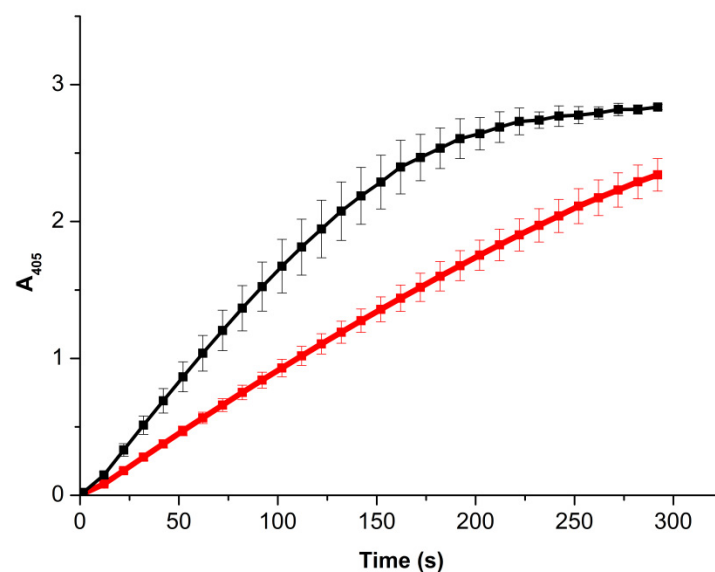


Figure 5. Results of spectrophotometry-based estimation of HRP enzymatic activity using a standard assay with ABTS. Typical time dependencies of the absorbance at 405 nm obtained for the HRP solution irradiated in PEMF (red curve), and for the control HRP solution (black curve). Experimental conditions: HRP:ABTS:H₂O₂ = 10^{−9} M:0.3 mM:2.5 mM. T = 23 °C.

The $A_{405}(t)$ curves shown in Figure 5 indicate that the enzymatic activity of HRP, whose solution was irradiated in PEMF for 40 min, decreased significantly (by 46%) in comparison with the control sample. In the case of shock wave impact, we did not observe any change in the enzymatic activity of HRP.

4. Discussion

As was noted in the introduction, in the development of novel diagnosticums intended for the registration of protein aggregation, and medicinal agents, aimed at the regulation of the aggregation process, it is important to study the factors, which influence the formation of protein aggregates. In the present research, the influence of pulsed electromagnetic and pressure fields with a very short rise-time of the front on the HRP enzyme protein has been investigated. Namely, the effect of a non-thermal sub-nanosecond-pulsed electromagnetic field on the aggregation state and functional activity of the enzyme has been studied. The results obtained indicate that a 640 kV/m pulsed electromagnetic field has a certain impact on the HRP enzyme: namely, an increased aggregation of the enzyme is observed after the 40 min incubation of its solution in this field. The change in the aggregation state of HRP, adsorbed onto mica from PEMF-irradiated samples, indicates an alteration in the surface structure of the protein globule, which leads to a change in the interactions between the HRP macromolecules with the mica surface, and with the solvent upon the adsorption. Namely, the following interactions take place in the near-surface layer of the AFM substrate upon adsorption of HRP macromolecules onto mica:

- (1) HRP monomer—HRP monomer;
- (2) HRP monomer—mica surface;
- (3) HRP monomer—solvent (buffer solution).

In addition, a change in the protein structure leads to an increase in the equilibrium constants of the above-listed processes. As a result, an increased aggregation of HRP occurs upon its adsorption onto mica.

Moreover, the changes in the HRP structure, induced by the action of PEMF, influenced the enzyme's active site conformation, and thus led to a significant (46%) reduction in the HRP functional activity.

Moreover, the impact of the pressure jump, induced by a fast rise-time (80 ns) shock wave with a duration of 4 ms, on the HRP enzyme was studied. It has been observed that such a pressure jump can cause a slight change in the HRP aggregation, pronounced in the form of an increase in the number of objects with 2 to 6 nm heights, which have not been observed in the control samples not exposed to the shock wave. That is, the effect of the pulsed pressure on the physicochemical properties of proteins has been shown. It should be noted that in the literature [6,30–33], the effect of a much higher (1000 to 3000 bar) constant pressure on the stereochemical properties of heme-containing enzymes was demonstrated. In this way, in [30,69], such studies with the example of cytochrome P450 were reported; therein, it was shown that, indeed, such an effect takes place, leading to a decrease in the spin state of heme iron in the substrate-bound enzyme—that is, a change in the enzyme's structure near its active site occurs. Analogous studies with the example of HRP were reported in [30,69], where it was demonstrated that an increased pressure leads to an increase in the rate of HRP association with carbon monoxide.

In our present study, we investigated the impact of a pressure jump within a narrow (10 atm) pressure range with a ~80 ns rise-time of the front and a short (~4 ms) duration. It was demonstrated that even within this pressure range at such short pulse durations, the pulsed pressure can lead to a change in the physicochemical properties of the enzyme, causing its tendency to aggregate upon adsorption onto mica.

External physicochemical impacts can also cause stereochemical changes in the structure of proteins. In particular, in heme-containing proteins, such changes can occur both in the structure of the globule and in the vicinity of the heme group, accompanying structural reconfigurations of the enzyme molecules. The study of changes in the stereochemical properties of molecules of heme-containing enzymes was carried out under such physicochemical impacts, as elevated temperature or addition of various substrates. In the literature, changes in the circular dichroism spectra of heme-containing proteins, including HRP, under the temperature and substrate influences during their catalytic cycle, were reported [70–73]. Namely, temperature variations cause changes in the functional activity of heme-containing proteins. Moreover, upon the interaction of HRP with a substrate during its catalytic cycle, even a change in the chirality in the spectral range, corresponding to the Soret band of the heme at 395 nm (where the positive sign of the circular dichroism spectrum changes to the negative one) is observed [72]. In our present study, we observed a significant decrease in the HRP activity after the impact of the picosecond PEMF. This can be explained by a change in the protein molecules' structure in the vicinity of the heme group and, possibly, by a corresponding change in the pseudo-chirality of the protein, expressed in the form of a change in the general structure of the (protein globule-heme) fold. Here, the term «pseudo-chirality» is used to define an incomplete mirror alignment of right-handed and left-handed structures, which is observed in many polymers, including proteins—in contrast to truly chiral small molecules [74]. This phenomenon is interesting to be studied in the future. An increase in the degree of aggregation of HRP upon its adsorption onto mica can also be accompanied by stereochemical changes. It is interesting to point out that the aggregation of some proteins can lead to a change in their circular dichroism spectra, as was demonstrated in the recently published paper [55] for lysozyme and chymotrypsin. Therein [55], a dependence of circular dichroism on the protein concentration—which is

known to lead to a change in the degree of aggregation of the protein in accordance with the dissociation constant K_d of the protein oligomerization reaction—was observed.

Regarding pressure impacts, it can cause stereochemical changes, leading to an increase in the binding of horseradish peroxidase with carbon monoxide, and shifting the spin equilibrium in another heme-containing enzyme, cytochrome P450—that is, causing structural changes in the heme site, as was reported in the literature [30,69]. In our present research, a short rise-time pulse of lower pressure leads to a change in protein aggregation, which also is expected to be connected with a change in the protein structure. As such, no change in the enzymatic functional activity of the protein is observed. This indicates an insignificant change in the protein structure away from its active site. Insignificant changes in the HRP structure, when the enzymatic activity remained unchanged, were also observed after the impact of weak knotted electromagnetic fields, as was demonstrated in our recent paper [64].

Our results reported herein indicate the effect of the impact of short pressure and electromagnetic pulses on the HRP enzyme. This effect consists in an increase in the degree of aggregation of the HRP enzyme upon its adsorption onto mica. Moreover, in the case of electromagnetic pulses, even a decrease in the enzymatic activity of HRP is observed. This can presumably cause stereochemical changes in the HRP structure—including the heme site, where, according to [72], a change in the pseudo-chirality can also be expected. Changes in stereochemical properties are planned to be investigated in future studies by other methods. Free hemin itself is optically inactive; at the same time, its presence within the protein globule leads to the appearance of chirality, accompanied by an appearance of a circular dichroism spectrum in the range corresponding to the Soret band wavelengths [72]. The chirality of proteins was shown to be important for not only programming the chirality of the globule-prosthetic group structure but also for programming the chirality of aggregates of protein with nanoparticles, which is not observed for individual protein-nanoparticle structures, making these aggregate structures optically active [74]. This opens up new conceptions regarding chirality in nature.

The effect of pulsed pressures and electromagnetic fields on enzymes, revealed with the example peroxidase solutions, should be taken into account in the development of models, describing physicochemical properties of proteins (in particular, the aggregation state) under the impact of external subnanosecond rise-time-pulsed electromagnetic fields and/or nanosecond rise-time-pulsed pressures. Various proteins, which are only functionally active in the oligomeric state, are known to provide proper functioning of the body. For instance, myeloperoxidase, which participates in inflammation-associated processes, is functionally active in the dimeric state [8], and destroying these dimers can lead to the occurrence of pathologies. Moreover, glutathione peroxidase, which participates in the regulation of oxidative stress in the body, is functionally active in the tetrameric state [10]. Another example is the FXR1 protein, which is involved in the regulation of memory and emotions [16]. However, protein oligomers are also known to be involved in the development of pathological processes in the body, such as cardiovascular [11] and oncological [12–15] diseases. This should be taken into account in the development of modern medical strategies aimed at correcting protein aggregation induced by the above-described factors. The study of such effects on the aggregation of not only the HRP enzyme but also other proteins is quite important for modeling pathological processes in the body. Moreover, protein aggregation can lead to hemodynamic obstructions in small vessels. This suggests that the influence of pulsed electromagnetic fields and pulsed pressures on the body should be monitored. The results obtained herein should also be taken into account in the development of novel highly sensitive diagnostic systems. Moreover, our results on the influence of pulsed pressure and electromagnetic fields on the interaction of mica with proteins are important to be taken into account in the development of novel methods intended for the early diagnosis of oncological diseases in humans.

5. Conclusions

The effect of picosecond rise-time electromagnetic radiation of non-thermal power on horseradish peroxidase enzyme has been studied. It has been demonstrated that such non-thermal-power radiation with a 640 kV/m field strength and a ~200 ps pulse rise-time can cause increased aggregation of the enzyme. As such, the enzymatic activity of HRP decreases by about 50%. In addition, it has been demonstrated that a pressure pulse with an 80 ns rise-time of the front can also lead to a change in the protein aggregation state. The results obtained herein are important for modeling the impact of pulsed picosecond electromagnetic radiation and pulsed pressure on the human body, as well as for further the development of radiation-shielding systems and safety standards regarding the practical use of these factors. Our results can also be of use in the development of novel highly sensitive medical diagnostic systems, intended for the early revelation of cancer in humans.

Author Contributions: Conceptualization, V.S.Z., V.Y.T., V.E.F. and Y.D.I.; data curation, I.D.S., A.F.K., D.I.L., A.N.E. and A.I.A. (Alexander I. Aleshko); formal analysis, A.N.E. and A.I.A. (Alexander I. Aleshko); funding acquisition, A.I.A. (Alexander I. Archakov); investigation, V.S.Z., T.O.P., I.D.S., A.F.K., A.A.V., I.A.I., M.O.E., A.N.E., V.Y.T., A.I.A. (Alexander I. Aleshko), K.Y.S., A.Y.D. and V.E.F.; methodology, K.Y.S., V.E.F. and Y.D.I.; project administration, Y.D.I.; resources, V.Y.T. and V.E.F.; software, D.I.L.; supervision, A.I.A. (Alexander I. Archakov); validation, V.E.F.; visualization, T.O.P., I.D.S., A.A.V. and M.O.E.; writing—original draft, T.O.P. and I.D.S.; writing—review and editing, Y.D.I. All authors have read and agreed to the published version of the manuscript.

Funding: The study was performed employing “Avogadro” large-scale research facilities, and was financially supported by the Ministry of Education and Science of the Russian Federation, Agreement No. 075-15-2021-933, unique project ID: RF00121X0004.

Data Availability Statement: Correspondence and requests for materials should be addressed to Y.D.I.

Conflicts of Interest: The authors declare no conflict of interest.

References

- Warille, A.A.; Altun, G.; Elamin, A.A.; Kaplan, A.A.; Mohamed, H.; Yurt, K.K.; Elhaj, A.E. Skeptical approaches concerning the effect of exposure to electromagnetic fields on brain hormones and enzyme activities. *J. Microsc. Ultrastruct.* **2017**, *5*, 177–184. [[CrossRef](#)] [[PubMed](#)]
- Moloney, B.M.; McAnena, P.F.; Abd Elwahab, S.M.; Fasoula, A.; Duchesne, L.; Gil Cano, J.D.; Glynn, C.; O’Connell, A.M.; Ennis, R.; Lowery, A.J.; et al. Microwave Imaging in Breast Cancer—Results from the First-In-Human Clinical Investigation of the Wavelia System. *Acad. Radiol.* **2021**, *5*, 1–12. [[CrossRef](#)]
- Zinoviev, S.V.; Evdokimov, A.N.; Sakharov, K.Y.; Turkin, V.A.; Aleshko, A.I.; Ivanov, A.V. Determination of therapeutic value of ultra-wideband pulsed electromagnetic microwave radiation on models of experimental oncology. *Meditsinskaya Fiz. Med. Phys.* **2015**, *3*, 62–67. Available online: https://www.researchgate.net/publication/282975692_Determination_of_Therapeutic_Value_of_Ultra-Wideband_Pulsed_Electromagnetic_Microwave_Radiation_on_Models_of_Experimental_Oncology (accessed on 29 November 2021).
- Jumaat, H.; Ping, K.H.; Abd Rahman, N.H.; Yon, H.; Redzwan, F.N.M.; Awang, R.A. A compact modified wideband antenna with CBCPW, stubline and notch-staircase for breast cancer microwave imaging application. *AEU-Int. J. Electron. Commun.* **2021**, *129*, 153492. [[CrossRef](#)]
- Karam, S.A.S.; O’Loughlin, D.; Oliveira, B.L.; O’Halloran, M.; Asl, B.M. Weighted delay-and-sum beamformer for breast cancer detection using microwave imaging. *Measurement* **2021**, *177*, 109283. [[CrossRef](#)]
- Mozhaev, V.V.; Heremans, K.; Frank, J.; Masson, P.; Balny, C. High Pressure Effects on Protein Structure and Function. *PROTEINS Struct. Funct. Genet.* **1996**, *24*, 81–91. [[CrossRef](#)]
- Ivanov, Y.D.; Pleshakova, T.O.; Shumov, I.D.; Kozlov, A.F.; Valueva, A.A.; Ivanova, I.A.; Ershova, M.O.; Larionov, D.I.; Repnikov, V.V.; Ivanova, N.D.; et al. AFM and FTIR Investigation of the Effect of Water Flow on Horseradish Peroxidase. *Molecules* **2021**, *26*, 306. [[CrossRef](#)] [[PubMed](#)]
- Gavrilenko, T.I.; Ryzhkova, N.A.; Parkhomenko, A.N. Myeloperoxidase and its role in development of ischemic heart disease. *Ukr. J. Cardiol.* **2014**, *4*, 119–126.
- Teng, N.; Maghzal, G.J.; Talib, J.; Rashid, I.; Lau, A.K.; Stocker, R. The roles of myeloperoxidase in coronary artery disease and its potential implication in plaque rupture. *Redox Rep.* **2017**, *22*, 51–73. [[CrossRef](#)] [[PubMed](#)]

10. Jacobson, G.A.; Yee, K.C.; Ng, C.H. Elevated plasma glutathione peroxidase concentration in acute severe asthma: Comparison with plasma glutathione peroxidase activity, selenium and malondialdehyde. *Scand. J. Clin. Lab. Investig.* **2007**, *67*, 423–430. [[CrossRef](#)] [[PubMed](#)]
11. Gouveia, M.; Xia, K.; Colón, W.; Vieira, S.I.; Ribeiro, F. Protein aggregation, cardiovascular diseases, and exercise training: Where do we stand? *Ageing Res. Rev.* **2017**, *40*, 1–10. [[CrossRef](#)] [[PubMed](#)]
12. Xu, J.; Reumers, J.; Couceiro, J.R.; De Smet, F.; Gallardo, R.; Rudyak, S.; Cornelis, A.; Rozenski, J.; Zwolinska, A.; Marine, J.C.; et al. Gain of function of mutant p53 by coaggregation with multiple tumor suppressors. *Nat. Chem. Biol.* **2011**, *7*, 285–295. [[CrossRef](#)]
13. Direito, I.; Monteiro, L.; Melo, T.; Figueira, D.; Lobo, J.; Enes, V.; Moura, G.; Henrique, R.; Santos, M.A.S.; Jerónimo, C.; et al. Protein Aggregation Patterns Inform about Breast Cancer Response to Antiestrogens and Reveal the RNA Ligase RTCB as Mediator of Acquired Tamoxifen Resistance. *Cancers* **2021**, *13*, 3195. [[CrossRef](#)]
14. Levy, C.B.; Stumbo, A.C.; Ano Bom, A.P.; Portari, E.A.; Cordeiro, Y.; Carneiro, Y.; Silva, J.L.; De Moura-Gallo, C.V. Co-localization of mutant p53 and amyloid-like protein aggregates in breast tumors. *Int. J. Biochem. Cell Biol.* **2011**, *43*, 60–64. [[CrossRef](#)] [[PubMed](#)]
15. Yang-Hartwich, Y.; Bingham, J.; Garofalo, F.; Alvero, A.B.; Mor, G. Detection of p53 Protein Aggregation in Cancer Cell Lines and Tumor Samples. In *Apoptosis and Cancer. Methods in Molecular Biology*; Mor, G., Alvero, A., Eds.; Humana Press: New York, NY, USA, 2015; Volume 1219. [[CrossRef](#)]
16. Sopova, J.V.; Koshel, E.I.; Belashova, T.A.; Zadorsky, S.P.; Sergeeva, A.V.; Siniukova, V.A.; Shenfeld, A.A.; Velizhanina, M.E.; Volkov, K.V.; Nizhnikov, A.A.; et al. RNA-binding protein FXR1 is presented in rat brain in amyloid form. *Sci. Rep.* **2019**, *9*, 18983. [[CrossRef](#)]
17. Benseny-Cases, N.; Álvarez-Marimon, E.; Aso, E.; Carmona, M.; Klementieva, O.; Appelhans, D.; Ferrer, I.; Cladera, J. In situ structural characterization of early amyloid aggregates in Alzheimer's disease transgenic mice and *Octodon degus*. *Sci. Rep.* **2020**, *10*, 5888. [[CrossRef](#)]
18. Zhang, X.; Fu, Z.; Meng, L.; He, M.; Zhang, Z. The early events that initiate β -amyloid aggregation in Alzheimer's disease. *Front. Aging Neurosci.* **2018**, *10*, 359. [[CrossRef](#)] [[PubMed](#)]
19. Morelli, A.; Ravera, S.; Panfoli, I.; Pepe, I.M. Effects of extremely low frequency electromagnetic fields on membrane-associated enzymes. *Arch. Biochem. Biophys.* **2005**, *441*, 191–198. [[CrossRef](#)]
20. Thumm, S.; Löschinger, M.; Glock, S.; Hämmerle, H.; Rodemann, H.P. Induction of cAMP-dependent protein kinase A activity in human skin fibroblasts and rat osteoblasts by extremely low-frequency electromagnetic fields. *Radiat. Env. Biophys.* **1999**, *38*, 195–199. [[CrossRef](#)]
21. Caliga, R.; Maniu, C.L.; Mihășan, M. ELF-EMF exposure decreases the peroxidase catalytic efficiency in vitro. *Open Life Sci.* **2016**, *11*, 71–77. [[CrossRef](#)]
22. Hamed, N.; Saviz, M.; Banaei, A.; Shabani, S.; Qafary, M.; Moosavi-Movahedi, A.A.; Faraji-Dana, R. Effects of circularly polarized electromagnetic fields on solvated hemoglobin structure. *J. Mol. Liq.* **2020**, *312*, 113283. [[CrossRef](#)]
23. Lopes, L.C.; Barreto, M.T.; Gonçalves, K.M.; Alvarez, H.M.; Heredia, M.F.; De Souza, R.O.M.; Cordeiro, Y.; Dariva, C.; Fricks, A.T. Stability and structural changes of horseradish peroxidase: Microwave versus conventional heating treatment. *Enzym. Microb. Technol.* **2015**, *69*, 10–18. [[CrossRef](#)]
24. Latorre, M.E.; Bonelli, P.R.; Rojas, A.M.; Gerschenson, L.N. Microwave inactivation of red beet (*Beta vulgaris* L. var. conditiva) peroxidase and polyphenoloxidase and the effect of radiation on vegetable tissue quality. *J. Food Eng.* **2012**, *109*, 676–684. [[CrossRef](#)]
25. Wasak, A.; Drozd, R.; Jankowiak, D.; Rakoczy, R. The influence of rotating magnetic field on bio-catalytic dye degradation using the horseradish peroxidase. *Biochem. Eng. J.* **2019**, *147*, 81–88. [[CrossRef](#)]
26. Emamdadi, N.; Gholizadeh, M.; Housaindokht, M.R. Investigation of static magnetic field effect on horseradish peroxidase enzyme activity and stability in enzymatic oxidation process. *Int. J. Biol. Macromol.* **2021**, *170*, 189–195. [[CrossRef](#)] [[PubMed](#)]
27. Gao, M.; Xie, Y.; Wang, S.; Shang, S.; Zhao, J.; Lu, X. A wideband picosecond pulsed electric fields (psPEF) exposure system for the nanoporation of biological cells. *Bioelectrochemistry* **2021**, *140*, 107790. [[CrossRef](#)] [[PubMed](#)]
28. Perelmuter, V.M.; Cha, V.A.; Chuprikova, E.M. *Medical and Biological Aspects of Interaction of Electromagnetic Waves with the Body*; Tomsk Polytechnic University: Tomsk, Russia, 2009.
29. Pleshakova, T.O.; Malsagova, K.A.; Kaysheva, A.L.; Kopylov, A.T.; Tatur, V.Y.; Ziborov, V.S.; Kanashenko, S.L.; Galiullin, R.A.; Ivanov, Y.D. Highly sensitive protein detection by biospecific AFM-based fishing with pulsed electrical stimulation. *FEBS Open Biol.* **2017**, *7*, 1186–1195. [[CrossRef](#)]
30. Hui Bon Hoa, G.; Douzou, P.; Dahan, N.; Balny, C. High-pressure spectrometry at subzero temperatures. *Anal. Biochem.* **1982**, *120*, 125–135. [[CrossRef](#)]
31. Eisenmenger, M.J.; Reyes-De-Corcuera, J.I. High pressure enhancement of enzymes: A review. *Enzym. Microb. Technol.* **2009**, *45*, 331–347. [[CrossRef](#)]
32. Andreou, V.; Dimopoulos, G.; Katsaros, G.; Taoukis, P. Comparison of the application of high pressure and pulsed electric fields technologies on the selective inactivation of endogenous enzymes in tomato products. *Innov. Food Sci. Emerg. Technol.* **2016**, *38*, 349–355. [[CrossRef](#)]
33. Akazawa, S.I.; Tokuyama, H.; Sato, S.; Watanabe, T.; Shida, Y.; Ogasawara, W. High-pressure tolerance of earthworm fibrinolytic and digestive enzymes. *J. Biosci. Bioeng.* **2018**, *125*, 155–159. [[CrossRef](#)]

34. Metzler, D.E. *Biochemistry, the Chemical Reactions of Living Cells*, 1st ed.; Academic Press: Cambridge, UK, 1977.
35. Davies, P.F.; Rennke, H.G.; Cotran, R.S. Influence of molecular charge upon the endocytosis and intracellular fate of peroxidase activity in cultured arterial endothelium. *J. Cell Sci.* **1981**, *49*, 69–86. [[CrossRef](#)]
36. Welinder, K.G. Amino acid sequence studies of horseradish peroxidase. amino and carboxyl termini, cyanogen bromide and tryptic fragments, the complete sequence, and some structural characteristics of horseradish peroxidase. *Cent. Eur. J. Biochem.* **1979**, *96*, 483–502. [[CrossRef](#)] [[PubMed](#)]
37. Ignatenko, O.V.; Sjölander, A.; Hushpulian, D.M.; Kazakov, S.V.; Ouporov, I.V.; Chubar, T.A.; Poloznikov, A.A.; Ruzgas, T.; Tishkov, V.I.; Gorton, L.; et al. Electrochemistry of chemically trapped dimeric and monomeric recombinant horseradish peroxidase. *Adv. Biosens. Bioelectron.* **2013**, *2*, 25–34.
38. Rogozhin, V.V.; Kutuzova, G.D.; Ugarova, N.N. Inhibition of horseradish peroxidase by N-ethylamide of o-sulfobenzoylacetic acid. *Russ. J. Bioorganic. Chem.* **2000**, *26*, 138–141. [[CrossRef](#)]
39. Veitch, N.C.; Smith, A.T. Horseradish peroxidase. *Adv. Inorg. Chem.* **2000**, *51*, 107–162.
40. Shannon, L.M.; Kay, E.; Lew, J.Y. Peroxidase isozymes from horseradish roots I. Isolation and physical properties. *J. Biol. Chem.* **1966**, *241*, 2166–2172. [[CrossRef](#)]
41. Tams, J.W.; Welinder, K.G. Mild chemical deglycosylation of horseradish peroxidase yields a fully active, homogeneous enzyme. *Anal. Biochem.* **1995**, *228*, 48–55. [[CrossRef](#)]
42. Pleshakova, T.O.; Bukharina, N.S.; Archakov, A.I.; Ivanov, Y.D. Atomic force microscopy for protein detection and their physicochemical characterization. *Int. J. Mol. Sci.* **2018**, *19*, 1142. [[CrossRef](#)] [[PubMed](#)]
43. Dufrêne, Y.F.; Ando, T.; Garcia, R.; Alsteens, D.; Martinez-Martin, D.; Engel, A.; Gerber, C.; Müller, D.J. Imaging modes of atomic force microscopy for application in molecular and cell biology. *Nat. Nanotechnol.* **2017**, *12*, 295–307. [[CrossRef](#)]
44. Uvarov, V.Y.; Ivanov, Y.D.; Romanov, A.N.; Gallyamov, M.O.; Kiselyova, O.I.; Yaminsky, I.V. Scanning tunneling microscopy study of cytochrome P450 2B4 incorporated in proteoliposomes. *Biochimie* **1996**, *78*, 780–784. [[CrossRef](#)]
45. Kiselyova, O.I.; Yaminsky, I.V.; Ivanov, Y.D.; Kanaeva, I.P.; Kuznetsov, V.Y.; Archakov, A.I. AFM study of membrane proteins, cytochrome P450 2B4, and NADPH-Cytochrome P450 reductase and their complex formation. *Arch. Biochem. Biophys.* **1999**, *371*, 1–7. [[CrossRef](#)]
46. Kuznetsov, V.Y.; Ivanov, Y.D.; Bykov, V.A.; Saunin, S.A.; Fedorov, I.A.; Lemeshko, S.V.; Hoa, H.B.; Archakov, A.I. Atomic force microscopy detection of molecular complexes in multiprotein P450cam containing monooxygenase system. *Proteomics* **2002**, *2*, 1699–1705. [[CrossRef](#)]
47. Archakov, A.I.; Ivanov, Y.D. Optical biosensor and scanning probe microscopy studies of cytochrome P450 interactions with redox partners and phospholipid layers. *Methods Enzymol.* **2002**, *357*, 94–103. [[CrossRef](#)]
48. Kuznetsov, V.Y.; Ivanov, Y.D.; Archakov, A.I. Atomic force microscopy revelation of molecular complexes in the multiprotein cytochrome P450 2B4-containing system. *Proteomics* **2004**, *4*, 2390–2396. [[CrossRef](#)] [[PubMed](#)]
49. Ramacviciene, A.; Snitka, V.; Mieliauskiene, R.; Ramanavicius, A. AFM-study of complement system assembly initiated by antigen-antibody complex. *Cent. Eur. J. Chem.* **2006**, *4*, 194–206. [[CrossRef](#)]
50. Archakov, A.I.; Ivanov, Y.D. Application of AFM and optical biosensor for investigation of complexes formed in P450-containing monooxygenase systems. *Biochim. Biophys. Acta-Proteins Proteom.* **2011**, *1814*, 102–110. [[CrossRef](#)] [[PubMed](#)]
51. Pleshakova, T.; Kaysheva, A.; Bayzyanova, J.; Anashkina, A.; Uchaikin, V.; Ziborov, V.; Konev, V.; Archakov, A.; Ivanov, Y. The detection of hepatitis C virus core antigen using AFM chips with immobilized aptamers. *J. Virol. Methods* **2018**, *251*, 99–105. [[CrossRef](#)]
52. Pleshakova, T.O.; Kaysheva, A.L.; Shumov, I.D.; Ziborov, V.S.; Bayzyanova, J.M.; Konev, V.A.; Uchaikin, V.F.; Archakov, A.I.; Ivanov, Y.D. Detection of hepatitis C virus core protein in serum using aptamer-functionalized AFM chips. *Micromachines* **2019**, *10*, 129. [[CrossRef](#)] [[PubMed](#)]
53. Kaysheva, A.L.; Pleshakova, T.O.; Stepanov, A.A.; Ziborov, V.S.; Saravanabhavan, S.S.; Natesan, B.; Archakov, A.I.; Ivanov, Y.D. Immuno-MALDI MS dataset for improved detection of HCVcoreAg in sera. *Data Brief.* **2019**, *25*, 104240. [[CrossRef](#)] [[PubMed](#)]
54. Usychenko, V.G.; Sorokin, L.N.; Usychenko, A.S. Penetration of Electromagnetic Radiation Energy into a Semiconductor Element Base of Technical Means without Specialized Receiving Antennas. *J. Commun. Technol. Electron.* **2020**, *65*, 1448–1456. [[CrossRef](#)]
55. Li, C.; Arakawa, T. Feasibility of circular dichroism to study protein structure at extreme concentrations. *Int. J. Biol. Macromol.* **2019**, *132*, 1290–1295. [[CrossRef](#)] [[PubMed](#)]
56. Sokolov, A.A.; Sakharov, K.Y.; Mikheev, O.V.; Turkin, V.A.; Aleshko, A.I. Radiators of ultrashort electromagnetic pulses. In Proceedings of the Third International Conference on Ultrawideband and Ultrashort Impulse Signals, Sevastopol, Ukraine, 18–22 September 2006; pp. 203–205. [[CrossRef](#)]
57. Podosenov, S.A.; Sakharov, K.Y.; Svekis, Y.G.; Sokolov, A.A. Linear two-wire transmission line coupling to an external electromagnetic field, Part II: Specific cases, experiment. *IEEE Trans. Electromagn. Compat.* **1995**, *37*, 566–574. [[CrossRef](#)]
58. Dobrotvorsky, M.I.; Sakharov, K.Y.; Mikheev, O.V.; Turkin, V.A.; Aleshko, A.I.; Dnischenko, V.N. Measuring instruments of powerful UWB EMP parameters. In Proceedings of the Third International Conference on Ultrawideband and Ultrashort Impulse Signals, Sevastopol, Ukraine, 18–22 September 2006; pp. 373–375. [[CrossRef](#)]
59. Sakharov, K.Y.; Turkin, V.A.; Mikheev, O.V.; Dobrotvorski, M.I.; Sukhov, A.V. A picosecond pulsed electric field strength measuring transducer. *Meas. Tech.* **2014**, *57*, 201–205. [[CrossRef](#)]
60. Gaydon, A.G.; Hurler, I.R. *The Shock Tube in High-Temperature Chemical Physics*; Reinhold Pub: Corp, NY, USA, 1963.

61. Ziborov, V.; Galiullin, R.; Efremov, V.; Shumova, V.; Fortov, V. Application of laser schlieren method for measurement of shock front structure in helium with small admixture of heavy molecules. *Bull. Mosc. Reg. State Univ. Ser. Phys. Math.* **2014**, *4*, 105–109.
62. Thomson, N.H. Imaging the substructure of antibodies with tapping-mode AFM in air: The importance of a water layer on mica. *J. Microsc.* **2005**, *217*, 193–199. [[CrossRef](#)] [[PubMed](#)]
63. Keller, D. Reconstruction of STM and AFM images distorted by finite-size tips. *Surface Sci.* **1991**, *253*, 353–364. [[CrossRef](#)]
64. Ivanov, Y.D.; Pleshakova, T.O.; Shumov, I.D.; Kozlov, A.F.; Ivanova, I.A.; Valueva, A.A.; Tatur, V.Y.; Smelov, M.V.; Ivanova, N.D.; Ziborov, V.S. AFM imaging of protein aggregation in studying the impact of knotted electromagnetic field on a peroxidase. *Sci. Rep.* **2020**, *10*, 9022. [[CrossRef](#)]
65. Ivanov, Y.D.; Pleshakova, T.O.; Shumov, I.D.; Kozlov, A.F.; Romanova, T.S.; Valueva, A.A.; Tatur, V.Y.; Stepanov, I.N.; Ziborov, V.S. Investigation of the Influence of Liquid Motion in a Flow-based System on an Enzyme Aggregation State with an Atomic Force Microscopy Sensor: The Effect of Water Flow. *Appl. Sci.* **2020**, *10*, 4560. [[CrossRef](#)]
66. Sanders, S.A.; Bray, R.C.; Smith, A.T. pH-dependent properties of a mutant horseradish peroxidase isoenzyme C in which Arg38 has been replaced with lysine. *Eur. J. Biochem.* **1994**, *224*, 1029–1037. [[CrossRef](#)]
67. Ivanov, Y.D.; Bukharina, N.S.; Frantsuzov, P.A.; Pleshakova, T.O.; Kanashenko, S.L.; Medvedeva, N.V.; Argentova, V.V.; Zgoda, V.G.; Munro, A.W.; Archakov, A.I. AFM study of cytochrome CYP102A1 oligomeric state. *Soft Matter* **2012**, *8*, 4602–4608. [[CrossRef](#)]
68. Chu, J.W.; Kimura, T. Studies on Adrenal Steroid Hydroxylases Molecular and catalytic properties of adrenodoxin reductase (a flavoprotein). *J. Biol. Chem.* **1973**, *248*, 2089–2094. [[CrossRef](#)]
69. Davydov, D.R.; Hui, B.; Hoa, G.; Peterson, J.A. Dynamics of protein-bound water in the heme domain of P450BM3 studied by high-pressure spectroscopy: Comparison with P450cam and P450 2B4. *Biochemistry* **1999**, *38*, 751–761. [[CrossRef](#)]
70. Chattopadhyay, K.; Mazumdar, S. Structural and conformational stability of horseradish peroxidase: Effect of temperature and pH. *Biochemistry* **2000**, *39*, 263–270. [[CrossRef](#)] [[PubMed](#)]
71. Sono, M.; Perera, R.; Jin, S.; Makris, T.M.; Sligar, S.G.; Bryson, T.A.; Dawson, J.H. The influence of substrate on the spectral properties of oxyferrous wild-type and T252A cytochrome P450-CAM. *Arch. Biochem. Biophys.* **2005**, *436*, 40–49. [[CrossRef](#)] [[PubMed](#)]
72. Strickland, E.H. Circular dichroism of horseradish peroxidase and its enzyme-substrate compounds. *Biochim. Biophys. Acta (BBA)-Enzymol.* **1968**, *151*, 70–75. [[CrossRef](#)]
73. Murugan, R.; Mazumdar, S. Role of substrate on the conformational stability of the heme active site of cytochrome P450cam: Effect of temperature and low concentrations of denaturants. *J. Biol. Inorg. Chem.* **2004**, *9*, 477–488. [[CrossRef](#)] [[PubMed](#)]
74. Efimov, A.V. Chirality and Handedness of Protein Structures. *Biochemistry* **2018**, *83*, S103–S110. [[CrossRef](#)] [[PubMed](#)]